

## Electronic surface states on the relaxed (111) surface of Ge

James R. Chelikowsky

*Bell Laboratories, Murray Hill, New Jersey 07974*

(Received 11 October 1976)

Self-consistent pseudopotentials are used to investigate the (111) surface of Ge. Using a relaxed surface, geometry comparisons are made with other calculational results for the Ge surface. In addition, the results for Ge are compared to recent calculations performed on the Si surface. Striking differences are found between Si and Ge for the dangling-bond energy dispersion curves and charge-density distributions. A generalized susceptibility calculation is performed for the Ge and Si surfaces. The results suggest a different reconstruction pattern for the two surfaces in only qualitative agreement with experiment.

### I. INTRODUCTION

The (111) Ge surface is investigated by means of a self-consistent pseudopotential calculation. At present there exist several pseudopotential<sup>1-3</sup> and tight-binding techniques<sup>4-6</sup> for determining the electronic structure of the surface region. These methods have been developed in large part because of the increasing experimental activity taking place on the field of semiconductor surfaces.

The first self-consistent pseudopotential calculation for a semiconductor surface was performed by Appelbaum and Hamann<sup>2</sup> (AH) in which they employed a mixed representation for the surface potential and solved Schrödinger's equation by direct numerical integration. The present method, on the other hand, involves imposing artificial periodicity on a slab geometry. By repeating slabs of the material of interest in a superlattice configuration, periodicity is retained and standard bulk pseudopotential techniques may be applied.

While these pseudopotential techniques have become fairly routine for a wide variety of surfaces and materials, a detailed comparison between them, and other techniques such as the tight-binding methods, has yet to be performed. In particular, the present Bloch-wave method has been criticized on the grounds that a large number of plane waves are required to describe the localized nature of surface-state wave functions. Thus, errors may be introduced into the method by an expansion in plane waves which is truncated too soon to yield accurate wave functions. To examine this problem in detail a comparison with another pseudopotential method, such as the AH method, which does not suffer from this problem, would be very useful.

However, it should be noted that while the AH method does not require a large number of plane waves to describe surface states, the present

technique does have certain advantages over this method. The present method, for example, is more flexible and simpler to use as compared to the AH technique. It does not require any new computational skills as it employs bulk pseudopotential ideas directly to the problem of the surface. In addition, it is capable of handling nonsurface problems, such as the electronic structure of vacancies or impurities in solids, in a straightforward fashion. Finally, unlike the AH technique, nonlocal pseudopotentials may be easily incorporated into the method. This latter point allows the method to be applied to systems outside of the AH method such as transition-metal surfaces.

The Ge (111) surface was chosen as a means of comparison because it exhibits some striking differences from the Si (111) surface. For example, while both surfaces exhibit a  $2 \times 1$  reconstruction upon cleaving, the Ge equilibrium reconstruction pattern corresponds to a  $2 \times 8$ ,<sup>7</sup> as contrasted to the Si  $7 \times 7$  pattern.<sup>8</sup> Furthermore, preliminary pseudopotential calculations<sup>9</sup> and some recent tight-binding results<sup>4,5</sup> have indicated radical differences existing in the energy dispersion curves for the dangling-bond surface states. These results produced a "double" pocket of occupied electron states for Ge as contrasted with the Si results indicating a single pocket.<sup>9</sup> Therefore, if Fermi-level instabilities play a role in forming the reconstruction patterns, the difference in the band dispersion should reflect the reconstruction differences.<sup>9,10</sup>

### II. METHOD OF CALCULATION

As mentioned above, the method involved in the calculation used the introduction of artificial periodicity into the system. As in the case of the (111) Si surface,<sup>1</sup> a 12-layer Ge slab was separated

by two bond lengths from its neighboring slabs in a superlattice configuration. The (111) surface is exposed on both sides of the slab. The slab thickness and separation between slabs is chosen to prevent any significant interactions between adjoining surfaces. With this crystal geometry, the wave functions may be written in Bloch form and solved by standard techniques.

A second crucial procedure employed in the method is the achievement of a self-consistent pseudopotential. A self-consistent response of the valence electrons is calculated for a fixed geometric arrangement of  $\text{Ge}^{4+}$  ionic potentials. The geometry assumed for the surface atoms has been discussed elsewhere,<sup>1,2,4</sup> and corresponds to a simple inward relaxation of the surface atoms. While this permits comparison between other methods, and allows us to assess differences between Ge and Si, it does prohibit a detailed comparison with experimental data on the observed reconstructed surfaces.

The ionic potentials are screened by using the valence charge density to compute Hartree and exchange potentials. The self-consistent process is initiated from an empirical potential

$$V(\vec{r}) = \sum_{\vec{G}} V_a(G) S(\vec{G}) \exp(i\vec{G} \cdot \vec{r}), \quad (1)$$

with

$$V_a(q) = a_1(q^2 - a_2) / \{ \exp[a_3(q^2 - a_4)] + 1.0 \}, \quad (2)$$

where  $\vec{G}$  corresponds to the reciprocal-lattice vectors of the superlattice,  $S(\vec{G})$  is the structure factor, and  $V_a(q)$  is an empirical atomic pseudopotential.<sup>1</sup> The values of the parameters  $a_i$  were chosen to replicate the energy spectrum for bulk Ge, and are listed in Table I.

With this initiating potential and fixed-surface atom geometry, the wave functions are expanded in terms of the reciprocal-lattice vectors  $\vec{G}$ . The eigenvectors and eigenfunctions are determined through a diagonalization of the secular equation.<sup>11</sup> Using the resulting wave functions, the total charge density can be calculated in terms of its Fourier coefficients  $\rho(\vec{G})$ . A Hartree potential can then be formed via Poisson's equation

$$V_H(\vec{G}) = (4\pi e^2 / \Omega_c) [\rho(\vec{G}) / G^2], \quad (3)$$

where  $\Omega_c$  is the cell volume of the superlattice. The exchange potential used is of the form

$$V_x(\vec{r}) = -\alpha (3/2\pi) (3\pi^2)^{1/3} e^2 [\rho(\vec{r})]^{1/3},$$

with  $\alpha = 0.8$ . The calculation of  $V_x$  requires an evaluation of  $\rho(\vec{r})$  throughout the unit cell. For this purpose,  $\rho(\vec{r})$  was evaluated on a grid of points (approximately  $10^3$  per unit cell), the cube root computed at each grid point, and the result trans-

TABLE I. Starting and ionic potential parameters as defined in Eqs. (2) and (4). If  $q$  is entered in atomic units, the resulting potential is in Ry.

	Potential parameters		
	Starting potential	Ionic potential	
$a_1$	9.7625	$Z$	4.0
$a_2$	2.3889	$\alpha$	0.61
$a_3$	0.610 98	$\nu_1$	2.64
$a_4$	-5.4917	$\nu_2$	-1.237

formed back into a Fourier series  $V_x(\vec{G})$ . To accurately compute the screening potentials, a special point sample scheme was used to calculate the required charge-density Fourier coefficients. A three-point special point scheme was used for this purpose.<sup>12,13</sup>

The sum of  $V_x(\vec{G})$  and  $V_H(\vec{G})$  was then added to the bare ion pseudopotential  $V_{\text{ion}}(q)$ . The Fourier coefficients for  $V_{\text{ion}}(q)$  may be obtained from the following:

$$V_{\text{ion}}(q) = \frac{1}{\Omega_c} \left[ -\frac{4\pi Z}{q^2} + \left(\frac{\pi}{\alpha}\right)^{3/2} \nu_1 + \left(\frac{\pi}{\alpha}\right)^{3/2} \times \left(\frac{3}{2\alpha} - \frac{q^2}{4\alpha^2}\right) \nu_2 \exp\left(\frac{-q^2}{4\alpha}\right) \right]. \quad (4)$$

This form was constructed from an ionic pseudopotential which accurately reproduces the atomic spectroscopic term values and, when self-consistently screened, the bulk energy spectrum for Ge.<sup>14</sup> Therefore, by continuity the ionic potential should adequately represent the surface ion potential. This ionic potential corresponds identically to those used in previous calculations.<sup>9</sup> The values of  $Z$ ,  $\alpha$ ,  $\nu_1$ , and  $\nu_2$  are given in Table I. The total potential

$$V_T(\vec{G}) = V_{\text{ion}}(G) S(\vec{G}) + V_H(\vec{G}) + V_x(\vec{G})$$

formed by the ionic potential plus the Hartree and exchange contributions, is then used to calculate new wave functions and screening potentials. By a systematic alteration of the input and output potentials, it is possible to obtain accurate agreement between the input and output potentials, and then achieve a self-consistent result. The self-consistent procedure therefore allows the valence charge to respond to fixed ion cores in a manner which involves *no* adjustable surface parameters.<sup>1,2</sup>

### III. RESULTS

In Fig. 1, the total self-consistent potential is displayed as a function of distance from deep within the slab to the center of the vacuum region.

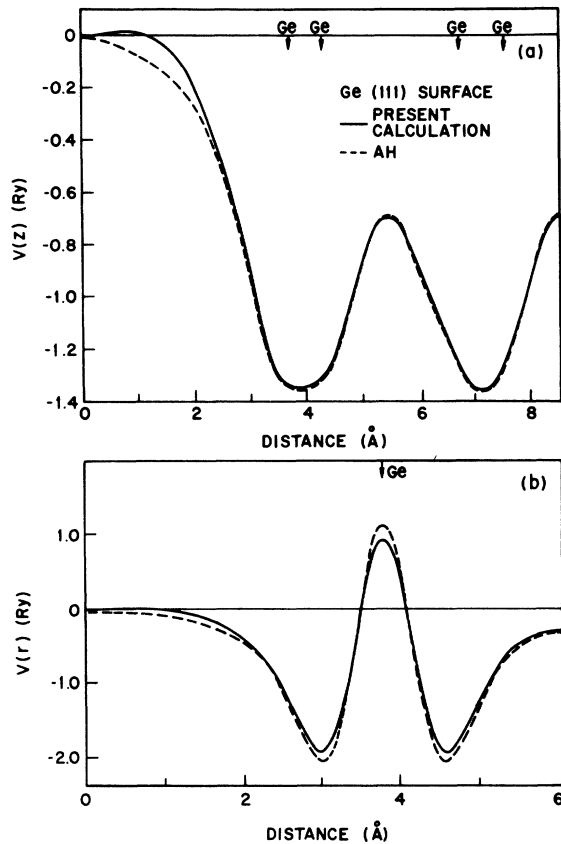


FIG. 1. Selfconsistent pseudopotential for the Ge(111) surface. In (a) the potential is averaged parallel to the (111) surface and plotted as a function of distance perpendicular to the surface. In (b) the potential is plotted as a ray plot through the outermost Ge ion. Also displayed are the results of Appelbaum and Hamann (Ref. 9).

Two cases are considered. In Fig. 1(a) the potential is averaged parallel to the surface, and in Fig. 1(b) it is plotted along a ray perpendicular to the surface, and through the surface atom. This slab potential is also compared to the result of AH's calculation.<sup>9</sup> The AH calculation is based on a semi-infinite geometry; however, in both calculations an identical core potential was used.

Because of the rather slow convergence for large  $\vec{q}$  vectors in (4), a large number of plane waves were used to expand the potential in the form indicated in (1). In obtaining the potential displayed in Fig. 1, approximately 1600 plane waves were used. Most of the differences in the present calculation and the AH result can be attributed to this fact. For example, the small deviations from AH's calculation occurring in the vacuum region are capable of being reduced by increasing the number of plane waves in the expansion. In Fig.

1(b) the present results exhibit differences from AH's calculation near the ion sites; the present potential does not become as repulsive nor as attractive as their potential. Again, this result is dependent on the number of waves used rather than differences between exchange potentials.<sup>1,2</sup>

In Fig. 2, the energy dispersion relations for surface states occurring in the optical gap, i.e., the dangling band states,<sup>1-5</sup> are displayed. A comparison is made with the results of the AH potential and the tight-binding results of Pandey and Phillips<sup>4</sup> (PP). The same type of dispersion for the energy band occurs in all three calculations. However, differences occur for the precise placement of this band. With respect to the present calculation, the AH result places the band approximately 0.2 eV lower in energy, whereas the PP result places it approximately 0.3 eV higher in energy. The 0.2-eV difference between our result and the AH result can probably be reduced by increasing the number of plane waves used in the basis.

Experimentally, there is some support for the position of the Fermi level as calculated by the pseudopotential techniques. Measurements on the

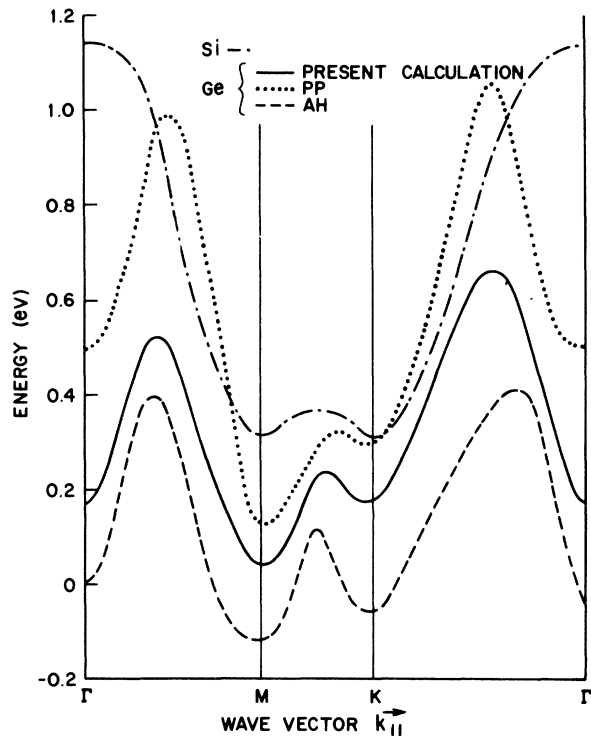


FIG. 2. Energy dispersion curves of the dangling-bond surface states for relaxed Ge and Si(111) surfaces. Also displayed for Ge are the results of Ref. 4 and Ref. 9.

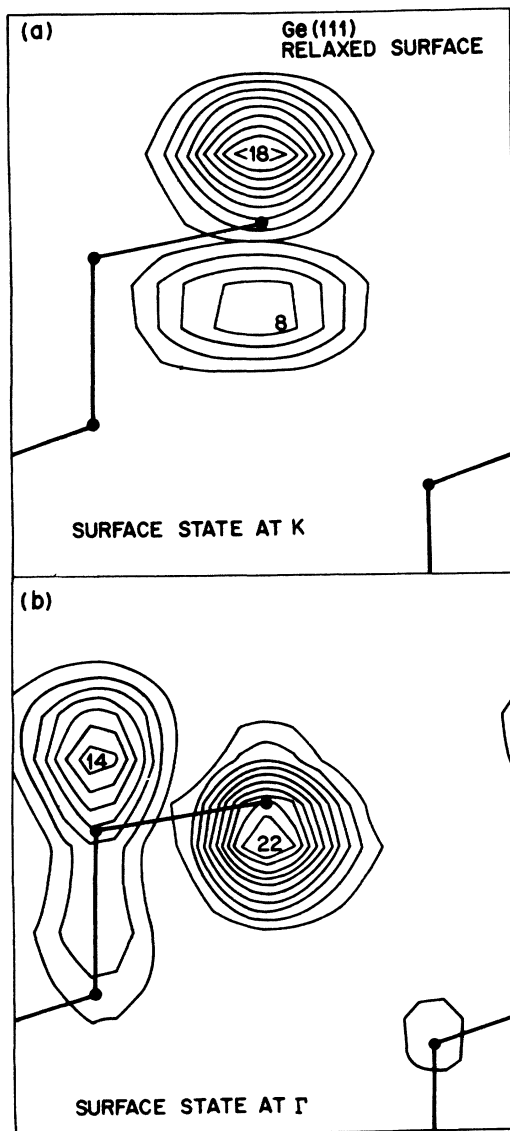


FIG. 3. Pseudocharge densities of the dangling-bond surface states for the relaxed Ge(111) surface. In (a) the charge density of  $K$  is displayed and in (b) the charge density at  $\Gamma$  is displayed. The contours are in units of electrons per unit cell volume.

annealed surfaces of Ge place the Fermi level in the lower portion of the optical gap near the valence band maximum.<sup>7,15</sup> The AH results place the Fermi level in this region as the dangling-bond band minimum actually occurs below the valence band edge. The present calculation also places the Fermi level in the lower half of the band gap, but the tight-binding results place the Fermi level at the mid-gap region or higher.<sup>4,5</sup>

In addition to obtaining a reasonable positioning

of the Fermi level, the present calculation also yields an accurate ionization potential. The calculated ionization potential is approximately 5.0 eV. This value is in accord with the experimental value of 4.9 eV for cleaved Ge.<sup>16</sup> The result is also compatible with recent work-function measurements of 4.8 and 4.6 eV obtained for the work function on cleaved and annealed surfaces, respectively.<sup>17</sup>

Compared to the dispersion of the dangling bond band of Ge, a Si relaxed surface<sup>1,2</sup> exhibits some strong differences. The dispersion curve for Si is displayed in Fig. 2. In the case of Si, the dangling bond band has a maximum at the zone center with local minima occurring at  $M$  and  $K$ . However, the Ge band has a minimum at the zone center, and the band maxima occur displaced away from the  $\Gamma$  point. This unusual result can be traced directly to the altered conduction band ordering in Ge as opposed to Si.<sup>18</sup> In Ge the antibonding conduction band  $\Gamma_2$  occurs nearly 3 eV lower with respect to the valence band maximum as compared to Si. The charge-density character of this band is found to strongly mix with the dangling bond states at  $\Gamma$ , altering the charge-density character and dispersion near the zone center. This effect is quite pronounced with respect to the charge density of states at the zone center.

In Fig. 3, the charge density for Ge is presented for the symmetry points  $K$  and  $\Gamma$ , for the dangling bond state. In Fig. 3(b), the charge at the zone center is displayed. The  $p$ -like lobes of this charge density are localized behind the first-layer surface atom and in front of the second-layer atom. This corresponds to localizing charge at the antibonding sites; however, the charge density at the zone edge has not been radically altered as is indicated in Fig. 3(a). This is in contrast to Si, where the charge density remains dangling-bond-like at both the zone center and zone edge and is similar to the Ge charge density illustrated in Fig. 3(a).

If we half occupy the dangling-bond band, as required by charge conservation, the effect of the charge character at the zone center upon the total charge density of the dangling-bond states is not appreciable. This result is a consequence of the small phase space of the electron pocket at the zone center. However, the additional charge localized on the second surface layer atoms by states occurring in the zone center could play a role in any adsorption process and might account for some differences observed between Si and Ge.<sup>19</sup>

With respect to the lower surface states, similar results as in the case of Si are obtained.<sup>1</sup> In particular the creation of surface states at the bottom

TABLE II. Fourier coefficients,  $E(\vec{k}) = \sum_{\vec{l}} \epsilon_{\vec{l}} \exp(i\vec{k} \cdot \vec{l})$ , for the expansion of the dangling-bond energy spectrum.  $\vec{l}$  is expressed in lattice coordinates,  $\vec{l} = n_1 \vec{b}_1 + n_2 \vec{b}_2$ , where  $\vec{b}_1$  and  $\vec{b}_2$  are the primitive reciprocal-lattice vectors. The energies are given in eV.

Fourier coefficients			
Si		Ge	
$\epsilon_{00}$	0.637	$\epsilon_{00}$	0.33
$\epsilon_{10}$	0.211	$\epsilon_{10}$	0.075
$\epsilon_{20}$	-0.027	$\epsilon_{20}$	-0.075
		$\epsilon_{21}$	-0.050

of the valence band occurs with relaxation as in the case of Si.<sup>1,2</sup> The calculated states are in approximate accord with tight-binding results,<sup>4,5</sup> and the energy loss experiments of Ludeke and Koma.<sup>15</sup> For example, at  $K$ , the tight-binding results of PP yield surface states at 8.9 and 5.6 eV below the valence band maximum (which correspond to the structure observed in the energy-loss measurements). This is compatible with the values calculated by the present pseudopotential method, which yields energies of 8.6 and 4.5 eV. The latter value is not in good accord with the PP results, but does agree with other tight-binding calculations.<sup>5</sup>

Finally, we calculate a generalized susceptibility<sup>10</sup> in order to assess the possibility of Fermi-level instabilities playing a role in the different reconstruction patterns observed for Si and Ge. The role of such instabilities has been discussed extensively in the literature<sup>9,10,20-26</sup>, and remains a controversial subject. It is, however, natural to assume that the differences occurring for the dangling bond spectrum between Si and Ge could play an important role. This speculation is reinforced by the close resemblance of the lower surface states and valence-band configuration of Ge and Si.

In an attempt to understand the relative differences between any Fermi-level reconstruction mechanisms between Si and Ge, we have evaluated the surface susceptibility  $\chi_s(\vec{q})$ ,

$$\chi_s(\vec{q}) = \sum_{\vec{k}_{11}} \frac{f_{\vec{k}_{11}}(1 - f_{\vec{k}_{11}+\vec{q}})}{(E_{\vec{k}_{11}} - E_{\vec{k}_{11}+\vec{q}})} \quad (5)$$

The  $f_{\vec{k}_{11}}$  are Fermi factors evaluated at  $T=0$ , and the  $E_{\vec{k}_{11}}$  correspond to the dangling-bond energies. Large values of  $\chi_s(\vec{q})$  at certain values of  $\vec{q}$  suggest the possibility of a surface reconstruction occurring with this wave vector. For example, a large value of  $\chi_s(\vec{q})$  for  $\frac{1}{2}\vec{q}_B$  would suggest a surface-unit cell reconstruction with twice the periodicity of an ideal surface.  $\chi_s(\vec{q})$  can be large when the

nesting of hole and electron pockets occurs as discussed elsewhere.<sup>10</sup> To evaluate the susceptibility,  $E_{\vec{k}_{11}}$  must be known throughout the zone. This was accomplished by expanding  $E_{\vec{k}_{11}}$  in a Fourier series. The coefficients are listed in Table II. The susceptibility was evaluated along high-symmetry lines by summing over a grid of approximately 2500  $\vec{k}_{11}$  points in the surface Brillouin zone. For both Ge and Si values of  $\vec{q}$  were found which significantly<sup>20</sup> exceeded  $\chi_s(q=0)$ . The results for both Ge and Si are presented in Fig. 4. In Fig. 5, the Fermi lines for the surfaces are indicated.

Experimentally both Ge and Si reconstruct upon annealing to higher order patterns than the observed  $2 \times 1$  low-energy-electron-diffraction (LEED) patterns obtained by cleaving.<sup>7,8</sup> The  $2 \times 1$  pattern changes to a  $2 \times 8$  for Ge, and a  $7 \times 7$  pattern for Si. The  $2 \times 8$  pattern of Ge is actually

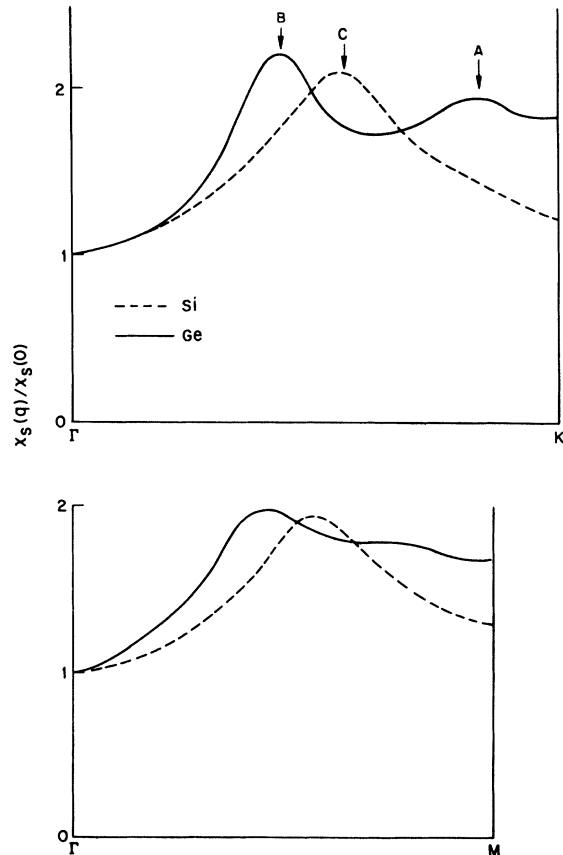


FIG. 4. Generalized susceptibility as defined in Eq. (5) for Ge and Si relaxed (111) surfaces. A, B, C label maxima which correspond to the vectors displayed in Fig. 5.

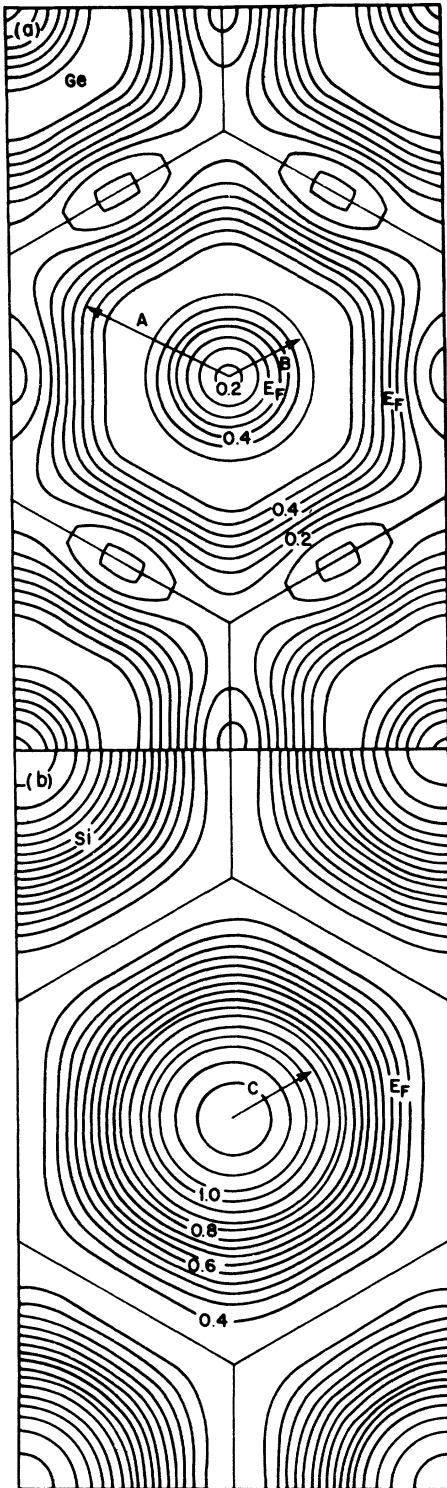


FIG. 5. Energy contour maps for the dangling-bond surface states for Ge and Si relaxed (111) surfaces. The contours are in steps of 0.05 eV. The vectors  $A$ ,  $B$ , and  $C$  displayed correspond to maxima in the susceptibility.

assumed to be composed of  $2 \times 8$  surface structure units which are randomly oriented about the three equivalent  $\langle 110 \rangle$  directions. Several models exist for these reconstructions based either upon the Haneman buckling model,<sup>24</sup> or the vacancy model of Lander.<sup>8</sup> In the Haneman model, the buckled  $2 \times 8$  is composed of  $2 \times 2$  units with appropriately altered rows of raised and lowered atoms.<sup>7</sup> In a similar fashion, Lander's model for the  $2 \times 8$  can be composed of  $2 \times 2$  cells with vacancies.<sup>7</sup>

In the case of Si, it has been argued that the Haneman model is more in accord with the  $2 \times 1$  reconstruction.<sup>21</sup> However, this point remains controversial,<sup>27</sup> and in the case of Ge, LEED data and oxidation data have been interpreted solely in terms of a Haneman model.<sup>16</sup>

In any event, the "nesting"  $\vec{q}$  vectors as calculated from the generalized susceptibility are indicated in Fig. 5. Qualitatively, the calculated results are in accord with experiment. In both Si and Ge a rather short vector occurs for which the value  $\chi_s(q)$  exhibits a strong peak. The length of the vector is, however, larger than what one would expect for a  $7 \times 7$  reconstruction, and would approximate *at best* a  $5 \times 5$  result. In the case of Ge, because of the zone center pocket, an additional longer vector exists. This vector nests the zone center pocket in the holelike lobe of the Fermi line occurring along the  $\Gamma - K$  direction, and is indicated by the subsidiary maximum in the susceptibility of Fig. 4. These results suggest the possibility of Ge reconstructing with a unit cell with one short dimension in contrast to Si and in agreement with LEED data.

#### IV. CONCLUSIONS

The relaxed (111) surface of Ge was investigated by means of a self-consistent pseudopotential scheme. A comparison with pseudopotential and tight binding techniques indicates general agreement between the results for the energy dispersion of the surface states within the band gap (i.e., the dangling-bond surface states). However, the energy placement of these states within the band gap for the various methods is not in good agreement. The pseudopotential results place these states within the lower-half of the optical gap, whereas the tight-binding results place these states within the upper-half of the gap.

A comparison between Si and Ge relaxed surfaces was also performed. The dangling bond states occurring for Si and Ge exhibit significant differences. In particular, the states existing near the zone center for Ge do not correspond to the classic dangling-bond charge distribution,<sup>2</sup> but rather correspond to charge distributions

which are localized along the antibonding directions. In addition, the Ge dangling-bond band exhibits dispersion which differs considerably from the equivalent Si surface. This result creates Fermi lines for the two surfaces which are quite different. Therefore, a generalized susceptibility calculation was performed to determine if nesting vectors exist which could account for the observed differences between the equilibrium reconstruction patterns of Si and Ge. The reconstructed

vectors determined in this fashion yielded patterns in only qualitative agreement with the LEED patterns.

#### ACKNOWLEDGMENTS

The author would like to thank J. A. Appelbaum and D. R. Hamann for very helpful comments and suggestions during the course of this work.

- 
- <sup>1</sup>M. Schluter, J. R. Chelikowsky, S. G. Louie, and M. L. Cohen, *Phys. Rev. Lett.* **34**, 1385 (1975); and *Phys. Rev. B* **12**, 4200 (1975).
- <sup>2</sup>J. A. Appelbaum and D. R. Hamann, *Rev. Mod. Phys.* (to be published).
- <sup>3</sup>A similar technique to Ref. 1 was developed by G. Alldredge and L. Kleinman [*Phys. Rev. Lett.* **28**, 1264 (1972)].
- <sup>4</sup>K. C. Pandey and J. C. Phillips, *Phys. Rev. Lett.* **32**, 1433 (1974); and *Phys. Rev. B* **13**, 750 (1976).
- <sup>5</sup>D. J. Chadi and M. L. Cohen, *Solid State Commun.* **16**, 691 (1975).
- <sup>6</sup>S. Ciraci, I. P. Batra, and W. A. Tiller, *Phys. Rev. B* **12**, 5811 (1975).
- <sup>7</sup>P. W. Palmberg and W. T. Peria, *Surf. Sci.* **6**, 57 (1967).
- <sup>8</sup>J. J. Lander and J. Morrison, *J. Appl. Phys.* **34**, 1403 (1963).
- <sup>9</sup>J. A. Appelbaum and D. R. Hamann, in *Physics of Semiconductors*, edited by M. Pilkuhn (Teubner, Stuttgart, 1974) p. 681.
- <sup>10</sup>E. Tosatti and P. W. Anderson, *Solid State Commun.* **14**, 773 (1974).
- <sup>11</sup>The convergence requirements, i.e., the number of plane waves used in the expansion of the wave functions and valence charge densities is discussed in Ref. 1.
- <sup>12</sup>D. J. Chadi and M. L. Cohen, *Phys. Rev. B* **8**, 5747 (1973).
- <sup>13</sup>S. L. Cunningham, *Phys. Rev. B* **10**, 4988 (1974).
- <sup>14</sup>J. A. Appelbaum and D. R. Hamann (unpublished).
- <sup>15</sup>R. Ludeke and A. Koma, *Phys. Rev. B* **13**, 739 (1976).
- <sup>16</sup>T. Murotani, K. Fujimara, and M. Nishijima, *Phys. Rev. B* **12**, 2424 (1976).
- <sup>17</sup>G. W. Gobeli and F. G. Allen, *Surf. Sci.* **2**, 402 (1964).
- <sup>18</sup>J. R. Chelikowsky and M. L. Cohen, *Phys. Rev. B* **10**, 5025 (1974).
- <sup>19</sup>M. Schluter, J. E. Rowe, G. Margaritondo, K. M. Ho, and M. L. Cohen, *Phys. Rev. Lett.* **37**, 1632 (1976).
- <sup>20</sup>J. A. Appelbaum, G. A. Baraff, and D. R. Hamann, *Phys. Rev. Lett.* **36**, 450 (1976).
- <sup>21</sup>J. E. Rowe and J. C. Phillips, *Phys. Rev. Lett.* **32**, 1315 (1974).
- <sup>22</sup>P. Ducros, *Surf. Sci.* **10**, 295 (1968).
- <sup>23</sup>L. Dobrzynski and D. C. Mills, *Phys. Rev. B* **7**, 2367 (1973).
- <sup>24</sup>D. Haneman, *Phys. Rev.* **121**, 1093 (1961).
- <sup>25</sup>J. C. Phillips, *Surf. Sci.* **40**, 459 (1973).
- <sup>26</sup>W. A. Harrison, *Surf. Sci.* **55**, 1 (1976).
- <sup>27</sup>E. Tosatti, *Festkorperprobleme* (Vieweg, Braunschweig, 1975), Vol XV, p. 113.